FOXO1-Mediated Downregulation of RAB27B Leads to Decreased Exosome Secretion in Diabetic Kidneys

Mengru Zeng,[1,2,3] Jin Wen,[2,3] Zhengwei Ma,[2,3] Li Xiao,[1] Yutao Liu,[2,3] Sangho Kwon,[2,3] Yu Liu,[1] and Zheng Dong[1,2,3]

Diabetes 2021;70:1536–1548 | https://doi.org/10.2337/db20-1108

Exosomes have been implicated in diabetic kidney disease (DKD), but the regulation of exosomes in DKD is largely unknown. Here, we have verified the decrease of exosome secretion in DKD and unveiled the underlying mechanism. In Boston University mouse proximal tubule (BUMPT) cells, high-glucose (HG) treatment led to a significant decrease in exosome secretion, which was associated with specific downregulation of RAB27B, a key guanosine-5′-triphosphatase in exosome secretion. Overexpression of RAB27B restored exosome secretion in HG-treated cells, suggesting a role of RAB27B downregulation in the decrease of exosome secretion in DKD. To understand the mechanism of RAB27B downregulation, we conducted bioinformatics analysis that identified FOXO1 binding sites in the Rab27b gene promoter. Consistently, HG induced phosphorylation of FOXO1 in BUMPT cells, preventing FOXO1 accumulation and activation in the nucleus. Overexpression of nonphosphorylatable, constitutively active FOXO1 led to the upregulation of RAB27B and an increase in exosome secretion in HG-treated cells. In vivo, compared with normal mice, diabetic mice showed increased FOXO1 phosphorylation, decreased RAB27B expression, and reduced exosome secretion. Collectively, these results unveil the mechanism of exosome dysfunction in DKD where FOXO1 is phosphorylated and inactivated in DKD, resulting in RAB27B downregulation and the decrease of exosome secretion.

Exosomes are single membrane-bound microvesicles containing nucleic acids, proteins, and lipids, which are formed in cells by an endosomal route and secreted to the extracellular milieu (1). A main cell biologic function of exosomes is to mediate intercellular communication. Exosomes have been implicated in various pathophysiological processes and diseases, such as mammalian development, infection and immune response, metabolic and cardiovascular diseases, neurodegeneration, cancer, and kidney disease (2–8).

There are two primary mechanisms for the biogenesis of exosomes, the endosomal sorting complex required for transport (ESCRT)-dependent pathway and the ESCRT-independent pathway (9). The ESCRT machinery consists of a series of cytosolic protein complexes, including ESCRT-0, ESCRT-I, ESCRT-II, and ESCRT-III, which facilitate the formation of multivesicular bodies (10). In contrast, the ESCRT-independent pathway mainly involves lipid raft-based microdomains for lateral segregation of cargos within the endosomal membrane. Regardless, the vesicles are finally excreted to the extracellular space via the fusion of multivesicular bodies with the plasma membrane. Exosome secretion is performed and regulated mainly by the RAB family of small guanosine-5′-triphosphatases (GTPases) and soluble NSF attachment protein receptor (SNARE) proteins (11). In this regard, RAB GTPases regulate exosome secretion by controlling various steps of intracellular vesicular trafficking, while SNARE proteins regulate exosome secretion via mediating the fusion of lipid bilayers (11).

As a common diabetic complication, diabetic kidney disease (DKD) is a leading cause of end-stage renal disease (ESRD) worldwide, bearing an enormous economic and health burden to patients, families, and the society (12–15). Considerable endeavors have been made to delineate the pathogenesis, discover biomarkers for early

[1]Department of Nephrology, The Second Xiangya Hospital, Central South University, Changsha, China
[2]Department of Cellular Biology and Anatomy, Medical College of Georgia at Augusta University, Augusta, GA
[3]Charlie Norwood VA Medical Center, Augusta, GA
Corresponding author: Zheng Dong, zdong@augusta.edu

Received 1 November 2020 and accepted 9 February 2021

This article contains supplementary material online at https://doi.org/10.2337/figshare.13812038.

See accompanying article, p. 1440.

diagnosis and progression prediction, and develop effective therapeutic interventions for DKD (16–24). Emerging research has implicated exosomes in DKD as a mode of intercellular communication. For example, Wu et al. (25) showed that exosomes from high-glucose (HG)-treated glomerular endothelial cells induced epithelial-mesenchymal transition and dysfunction in cultured podocytes. Zhu et al. (26) reported that exosomes from HG-treated macrophages activated glomerular mesangial cells via the transforming growth factor (TGF)-β1/Smad3 pathway in vitro and in vivo. Exosomes from HG-treated macrophages could activate macrophages via the nuclear factor (NF)-κB pathway (27). Su et al. (28) further demonstrated that exosomes from podocytes mediated the dedifferentiation of renal proximal tubule cells via miRNA-221 in DKD models. Other studies suggested beneficial effects of stem cells-derived exosomes in the treatment of DKD and role as biomarkers of urinary exosomes in DKD (29–36). Despite these studies, very little is known about the regulation of exosome biogenesis and secretion in DKD.

Our recent study demonstrated a significant reduction in exosome secretion in HG-treated renal tubular cells and in renal cortical tissues of Akita diabetic mice (37). The current study has verified this finding and further investigated the molecular mechanism leading to decreased exosome secretion in DKD. Our results show that in diabetic kidney cells and tissues, FOXO1 is phosphorylated and inactivated, resulting in the downregulation of RAB27B and the decrease of exosome secretion. These findings provide new insights into exosome regulation in the pathogenesis of DKD.

RESEARCH DESIGN AND METHODS

Antibodies and Special Reagents

Antibodies were purchased from the following sources: anti-ALIX and anti-TSG101 antibodies from Santa Cruz Biotechnology (Dallas, TX); anti-CD63 and anti–α-tubulin antibodies from Abcam (Cambridge, MA); anti-FOXO1, anti–phosphorylated (p)-FOXO1 (Ser256), anti-cyclophilin B, anti-GAPDH, and anti-histone H3 antibodies from Cell Signaling Technology (Danvers, MA); anti–β-actin antibody from Sigma-Aldrich (St. Louis, MO); anti-RAB27A and anti-RAB27B antibodies from Proteintech (Chicago, IL); and all secondary antibodies from Jackson ImmunoResearch (West Grove, PA). Special reagents were purchased from the following sources: Foxo1 siRNA and scrambled siRNA from Cell Signaling Technology, Rab27b plasmid from OriGene Technologies (Rockville, MD), nonphosphorylatable, constitutively active Foxo1 plasmid from Addgene (Cambridge, MA) (38), exosome-depleted FBS from Thermo Fisher Scientific (Waltham, MA), streptozotocin (STZ) from Sigma-Aldrich, and recombinant human TGF-β1 from R&D Systems (Minneapolis, MN).

Cell Culture and HG Incubation

The Boston University mouse proximal tubular cell line (BUMPT) was originally obtained from Dr. Wilfred Lieberthal (Boston University School of Medicine, Boston, MA) (39). We established a stably transfected BUMPT cell line overexpressing RAB27B with the Rab27b plasmid and a stably transfected BUMPT cell line overexpressing nonphosphorylatable FOXO1 with the plasmid of constitutively active Foxo1. The human proximal tubular HK-2 cell line was from ATCC (CRL-2190). BUMPT cells and HK-2 cells were cultured in media containing HG (30 mmol/L glucose) or normal glucose (NG; 5.5 mmol/L glucose + 24.5 mmol/L D-mannitol) for 8 days, as previously described (37). Briefly, medium with 10% FBS was refreshed on the 3rd and 5th day. On the 7th day, cells were changed to serum-free medium. After 24 h, the medium was changed to serum-free medium again. Cell culture medium was collected at the end of the 8th day for exosome isolation.

Isolation and Identification of Exosomes From Cell Culture Medium

Exosomes were isolated from collected cell culture medium by centrifugation and ultracentrifugation, as previously described (37). The exosome pellets were lysed for immunoblot analysis of exosome marker proteins or resuspended in particle-free PBS for nanoparticle tracking analysis (NTA).

Diabetic Mouse Models

Animal work was conducted according to a protocol approved by the Institutional Animal Care and Use Committee of Charlie Norwood VA Medical Center (Augusta, GA). C57BL/6 male mice (7 weeks) from The Jackson Laboratory were treated with 50 mg/kg/day STZ for 5 days to induce type 1 diabetes (T1DM), as previously described (40). Mice with a fasting blood glucose >200 mg/dL were considered diabetic. In addition, $Ins2^{Akita}$ mice were used for T1DM. Obese *db/db* mice were used as a model of type 2 diabetes, and their lean littermates (*db/m*) served as nondiabetic controls. Mice were sacrificed at 20–22 weeks of age.

Isolation of Exosomes From Mouse Renal Cortical Tissues

Exosomes were isolated from 10 mg of mouse renal cortical tissues by digestion, centrifugation, filtration, and ultracentrifugation, as previously described (37). The exosome pellets were resuspended in particle-free PBS for NTA.

NTA

NTA was performed with ZetaView (Particle Metrix, Mebane, NC) to measure the size, distribution, and concentration of exosomes, as previously described (37). The concentration of exosomes was normalized with the corresponding cell count. The cell count was measured using

a TC20 Automated Cell Counter after the cells in each dish were digested into suspension by trypsin at the end of treatment.

Immunoblot Analysis

Proteins were separated by 10% SDS-PAGE and analyzed by immunoblot using the method as previously described (37).

Cell Transfection

Rab27b and nonphosphorylatable, constitutively active Foxo1 were subcloned into the pcDNA4/TO vector (Addgene). For transient transfection, cells were transfected with 1 μg plasmids using Lipofectamine 2000 (Invitrogen, Waltham, MA). For stable transfection, cells were transfected with 1 μg plasmid DNA using Lipofectamine 2000, followed by 2 weeks of selection with 500 μg/mL Zeocin (Invitrogen).

Subcellular Fractionation

Cells were rinsed with cold PBS and scraped in 500 μL PBS with 0.1% NP-40. The cell lysates were centrifuged at 13,000*g* for 30 s to collect supernatant as the cytoplasmic fraction. The pellet was washed with PBS with 0.1% NP-40, collected by centrifugation, and resuspended in Laemmli buffer as the nuclear fraction.

Quantitative Real-Time PCR Analysis

Quantitative real-time PCR analysis was performed using the method as previously described (15). Primer sequences of β-actin and Rab27b were as follows: mouse β-actin (forward: 5′-GGCTGTATTCCCCTCCATCG-3′, reverse: 5′-CCAGTTGGTAACAATGCCATGT-3′); human β-actin (forward: 5′-CATGTACGTTGCTATCCAGGC-3′, reverse: 5′-CTCCTTAATGTCACGCACGAT-3′); mouse Rab27b (forward: 5′-CGTCAGGAAAAGCGTTTAAGGT-3′, reverse: 5′-AGAAGCTCTGTTGACTGGTGA-3′); and human Rab27b (forward: 5′-TAGACTTTCGGGAAAAACGTGTG-3′, reverse: 5′-AGAAGCTCTGTTGACTGGTGA-3′).

Chromatin Immunoprecipitation Assay

Chromatin immunoprecipitation (ChIP) assay was performed using the method as previously described (15). The DNA samples were analyzed by real-time PCR with input DNA for normalization using primers designed according to the FOXO1 binding site sequence in the Rab27b gene (forward: 5′-CGGAAAGACAGTTTGGTGATAAAG-3′, reverse: 5′-TCAAGCCTAGCCTATTCTGTT T-3′).

Immunohistochemistry and Histological Staining

Kidney tissues were fixed in 4% paraformaldehyde, embedded in paraffin, and then sectioned at 4 μm. For immunohistochemistry, tissue sections were subjected to rehydration, antigen retrieval, and incubation in blocking buffer containing 2% BSA, 0.2% milk, and 2% normal goat serum in PBS with 0.8% Triton X-100. Tissue sections were then exposed to the primary antibody overnight at 4°C, followed by incubation with the horseradish peroxidase-conjugated secondary antibody (DAKO, Carpinteria, CA) for 1 h at room temperature. The sections were finally developed with VECTASTAIN Elite ABC kit and ImmPACT DAB peroxidase substrate (Vector Laboratories, Burlingame, CA). Quantification analysis was performed by Image-Pro Plus software (Media Cybernetics, Rockville, MD). For periodic acid Schiff staining, tissue sections were oxidized in 1% periodic acid solution for 10 min, rinsed in distilled water, and then incubated in Schiff's solution for 10 min. The slides were rinsed in metabisulfite solution and washed in running water, followed by counterstaining with hematoxylin. Sirius Red/Fast Green collagen staining was performed according to the manufacturer's instructions using the Sirius Red/Fast Green collagen staining kit from Chondrex (Woodinville, WA). Quantification was performed by Image-Pro Plus software.

Statistics

Data are expressed as mean ± SD. Statistical analysis was performed using GraphPad Prism software (GraphPad Software, San Diego, CA). Significant differences between groups were tested by the Student *t* test when there were only two groups. For more than two groups, significant differences between groups were determined by one-way ANOVA. Differential Rab27b mRNA expression in the glomerulus and tubulointerstitium between healthy donors and DKD patients was obtained from the Nephroseq v5 online platform (https://v5.nephroseq.org). The Pearson correlation analysis between Rab27b mRNA expression in the tubulointerstitium and estimated glomerular filtration rate (eGFR) based on the MDRD equation in human diabetic kidneys was also performed using the Nephroseq v5 online platform. $P < 0.05$ (two-sided) was considered statistically significant.

Data and Resource Availability

The data of this study are available on request.

RESULTS

HG Incubation Reduces Exosome Secretion in Renal Tubular Cells

BUMPT cells and HK-2 cells were cultured in media containing HG (30 mmol/L glucose) or NG (5.5 mmol/L glucose + 24.5 mmol/L D-mannitol) for 8 days. The media were collected at the end of the 8th day for exosome isolation and analysis. To characterize the isolated exosomes, we performed NTA (Fig. 1*A*) and immunoblot analysis of exosome marker proteins, including ALIX, CD63, and TSG101 in the NG and HG groups from an equal number of cells (Fig. 1*B*). The results showed that the peak diameter of extracted exosomes was ∼120 nm and that the protein levels of ALIX, CD63, and TSG101 in the HG group were lower than those in the NG group. Interestingly,

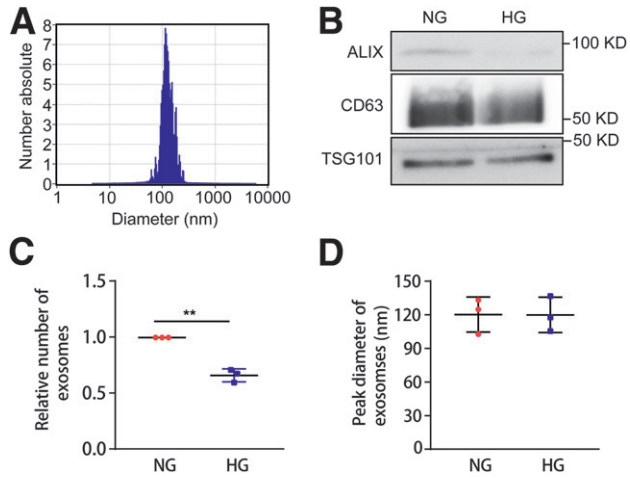

Figure 1—HG incubation reduces exosome secretion in BUMPT cells. BUMPT cells were cultured in DMEM containing 30 mmol/L glucose (HG) or 5.5 mmol/L glucose with 24.5 mmol/L D-mannitol (NG) for 8 days as detailed in *Research Design and Methods*. Cell culture medium was collected at the 8th day for exosome isolation and further analysis. *A*: NTA of isolated exosomes from the HG condition. *B*: Immunoblot analysis of exosome marker proteins, including ALIX, CD63, and TSG101. Exosome samples collected from an equal number of cells in the NG and HG groups were analyzed. *C*: HG incubation reduced exosome secretion. Exosomes were quantified by NTA, and the exosome number was then normalized with the cell numbers in the NG and HG groups ($n = 3$). $^{**}P < 0.01$. *D*: HG treatment did not change the size of exosomes. Peak diameter of exosomes was analyzed by NTA in the NG and HG groups ($n = 3$).

HG-treated BUMPT cells and HK-2 cells produced fewer exosomes, whereas there was no significant change in the size of exosomes (Fig. 1*C* and *D* and Supplementary Fig. 1*A* and *B*). These data indicate that HG incubation reduces exosome secretion in renal tubular cells.

RAB27B Is Specifically Downregulated in HG-Treated Cells

We then investigated the molecular mechanisms regulating exosome secretion under diabetic condition. Immunoblot analysis was performed to examine the expression of several key proteins involved in exosome biogenesis and secretion, such as ALIX, TSG101, RAB27A, and RAB27B (Fig. 2*A*–*E* and Supplementary Fig. 1*C*–*G*). The results showed a significant and specific decrease in RAB27B expression after HG incubation. We further analyzed the mRNA level of Rab27b from cell lysates in the NG and HG groups by real-time PCR (Fig. 2*F* and Supplementary Fig. 1*H*), revealing that the mRNA level of Rab27b in the HG group was significantly lower than that in the NG group. The results indicate that HG incubation downregulates RAB27B at the gene transcription level in renal tubular cells.

RAB27B Downregulation Contributes to Decreased Exosome Secretion in HG-Incubated Cells

To investigate whether RAB27B repression was responsible for decreased exosome secretion in HG-incubated cells, we generated stable, RAB27B-overexpressing BUMPT cells. Immunoblot analysis showed that stable transfection of Rab27b in BUMPT cells led to significantly higher expression of RAB27B compared with that of empty vector-transfected cells (Fig. 3*A* and *B*). We performed NTA to analyze the number and size of exosomes secreted by these cells in the absence or presence of HG incubation. As expected, HG reduced exosome secretion. RAB27B overexpression increased exosome secretion in both NG-treated and HG-treated cells (Fig. 3*C*). In contrast, RAB27B overexpression did not significantly change in the size of exosomes (Fig. 3*D*). Together, these data suggest that RAB27B is a critical factor for exosome secretion and that its downregulation in HG-treated cells contributes to the decreased exosome secretion in these cells.

Regulation of RAB27B by FOXO1 in BUMPT Cells

We next investigated how RAB27B was downregulated by HG exposure. Because the downregulation was associated with a significant decrease in mRNA expression (Fig. 2*F*), we focused on the transcription mechanism. We first analyzed the Rab27b gene promoter with the JASPAR database (https://jaspar.genereg.net), which identified the most potential FOXO1 binding site in the mouse Rab27b gene promoter region (Fig. 4*A*). The FOXO1 binding site was identical in mouse and rat and was partially conserved in human (Fig. 4*B*). Notably, FOXO1 is an important transcription factor involved in renal tubulointerstitial fibrosis in DKD (41,42).

To determine whether RAB27B can be regulated by FOXO1, we examined the effects of FOXO1 knockdown and overexpression. Transient transfection of Foxo1 siRNA (siFoxo1) attenuated FOXO1 expression in BUMPT cells (Fig. 4*C* and *D*). Importantly, RAB27B expression was significantly reduced in FOXO1 knockdown cells (Fig. 4*C* and *E*), indicating the regulation of RAB27B by FOXO1.

FOXO1 is negatively regulated by phosphorylation. Specifically, phosphorylation of FOXO1 at T24, S256, and S319 sites prevents its accumulation in the nucleus and results in its inactivation. Accordingly, mutation of these sites to nonphosphorylatable residuals results in constitutively active FOXO1 (38,43). In our study, transfection of nonphosphorylatable, constitutively active Foxo1 led to an increase in RAB27B expression in BUMPT cells (Fig. 4*F* and *H*), further indicating that FOXO1 is an upstream inducer of RAB27B in renal tubular cells.

HG Induces FOXO1 Phosphorylation and Inactivation in BUMPT Cells

There is evidence that FOXO1 is phosphorylated and inactivated in DKD (44). Our results shown above in Fig. 4 suggest FOXO1 may be an upstream regulator of RAB27B. We therefore hypothesized that FOXO1 phosphorylation and inactivation in DKD leads to RAB27B downregulation for decreased exosome secretion. To test this possibility, we initially verified that HG incubation induced FOXO1 and

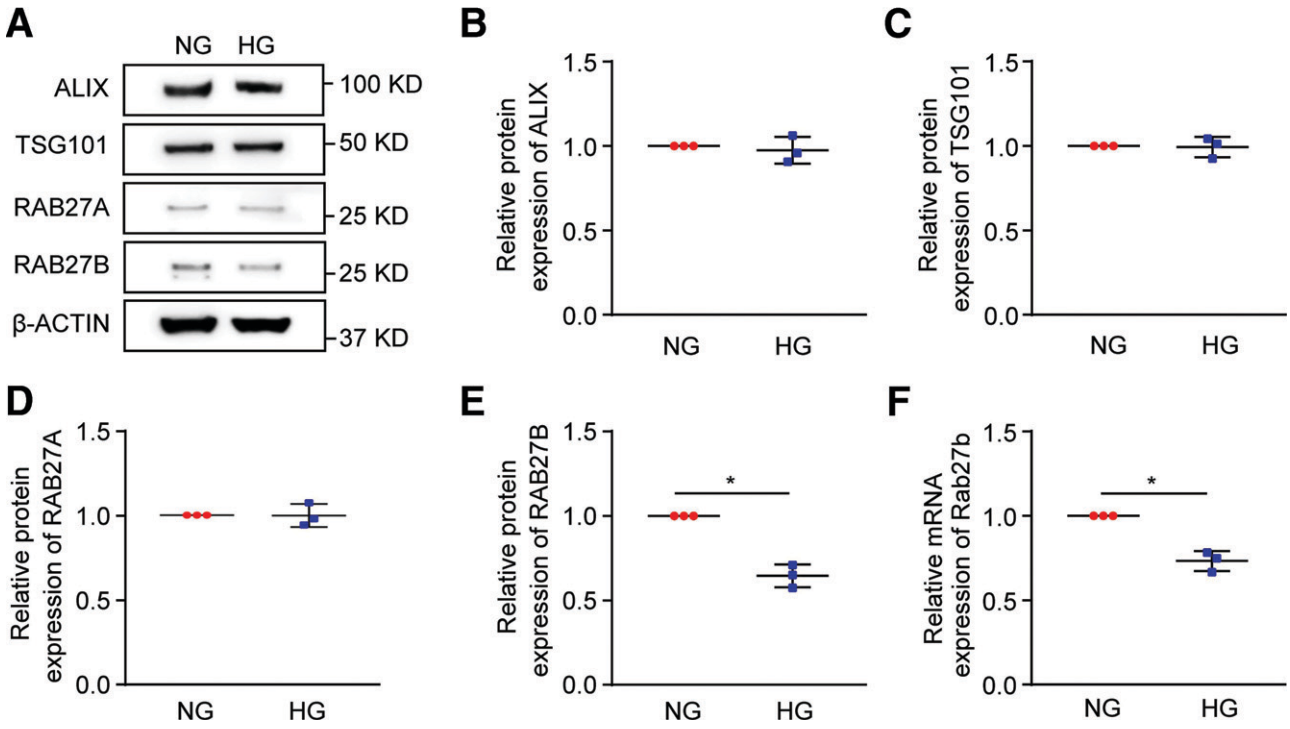

Figure 2—RAB27B is specifically downregulated in HG-treated BUMPT cells. BUMPT cells were cultured in DMEM containing 30 mmol/L glucose (HG) or 5.5 mmol/L glucose with 24.5 mmol/L D-mannitol (NG). Cell lysates were collected for immunoblot analysis. *A*: Decreased protein level of RAB27B in HG-treated cells. Representative immunoblots of ALIX, TSG101, RAB27A, and RAB27B from cell lysates in the NG and HG groups. Densitometric analyses of ALIX (*B*), TSG101 (*C*), RAB27A (*D*), and RAB27B (*E*) from cell lysates in the NG and HG groups. β-Actin was used as the loading control. After normalization with β-actin, the protein level in the NG group was arbitrarily set as 1, and the protein level in the HG group was compared with it to calculate the fold change. $*P < 0.05$ ($n = 3$). *F*: Decreased mRNA level of Rab27b in HG-treated cells. The mRNA level of Rab27b was detected by real-time PCR with β-actin as the reference gene. After normalization with β-actin, the mRNA level in the NG group was arbitrarily set as 1, and the mRNA level in the HG group was compared with it to calculate the fold change. $*P < 0.05$ ($n = 3$).

FOXO1 phosphorylation in BUMPT cells, although the induction was not dramatic (Fig. 5*A–C*). We further analyzed nuclear translocation of FOXO1 by fractionation of the cells. As shown in Fig. 5*D–F*, in normal glucose cells, most of the FOXO1 was detected in the cytosol, but some was in the nucleus. Upon HG treatment, nuclear accumulation of FOXO1 was partially reduced, whereas cytosolic FOXO1 was increased. Taken together, these data indicate that HG induces FOXO1 phosphorylation and inhibits FOXO1 nuclear translocation or activation in renal tubular cells.

Regulation of RAB27B by FOXO1 Reduces Exosome Secretion in HG-Incubated BUMPT Cells

To determine whether the regulation of RAB27B by FOXO1 reduces exosome secretion in BUMPT cells under the HG condition, we examined the effects of overexpressing nonphosphorylatable, constitutively active FOXO1. As shown in Fig. 6*A–D*, overexpression of active FOXO1 in BUMPT cells reduced FOXO1 phosphorylation and significantly increased the expression of RAB27B in both NG-treated and HG-treated cells. NTA detected a decrease of exosome secretion after HG incubation of BUMPT cells, and remarkably, this decrease was attenuated in FOXO1 overexpressing cells. Of note, active FOXO1 dramatically increased exosome secretion in both NG-treated and HG-treated cells, whereas it did not affect the size of exosomes (Fig. 6*E* and *F*). To verify FOXO1 binding to the predicted site of the Rab27b promoter (Fig. 4*A*), ChIP assay was performed. As shown in Fig. 6*G*, HG incubation induced a 26.7% decrease in FOXO1 binding to the Rab27b promoter sequence. These data suggest that downregulation of RAB27B by FOXO1 contributes to reduced exosome secretion during HG incubation of renal tubular cells.

FOXO1 Inactivation and RAB27B Repression Are Associated With Decreased Exosome Secretion in DKD Mice

To verify the FOXO1/RAB27B pathway of exosome regulation in vivo, we analyzed DKD in mouse models of T1DM and type 2 diabetes. Renal cortical tissues were collected at 20 weeks after the STZ injection. As shown in Supplementary Fig. 2, STZ-treated mice had lower body weight, higher fasting blood glucose, worse renal tubular damage, and more severe interstitial fibrosis compared with nondiabetic controls. NTA detected fewer exosomes (30.7% decrease vs. control) in renal cortical tissues of

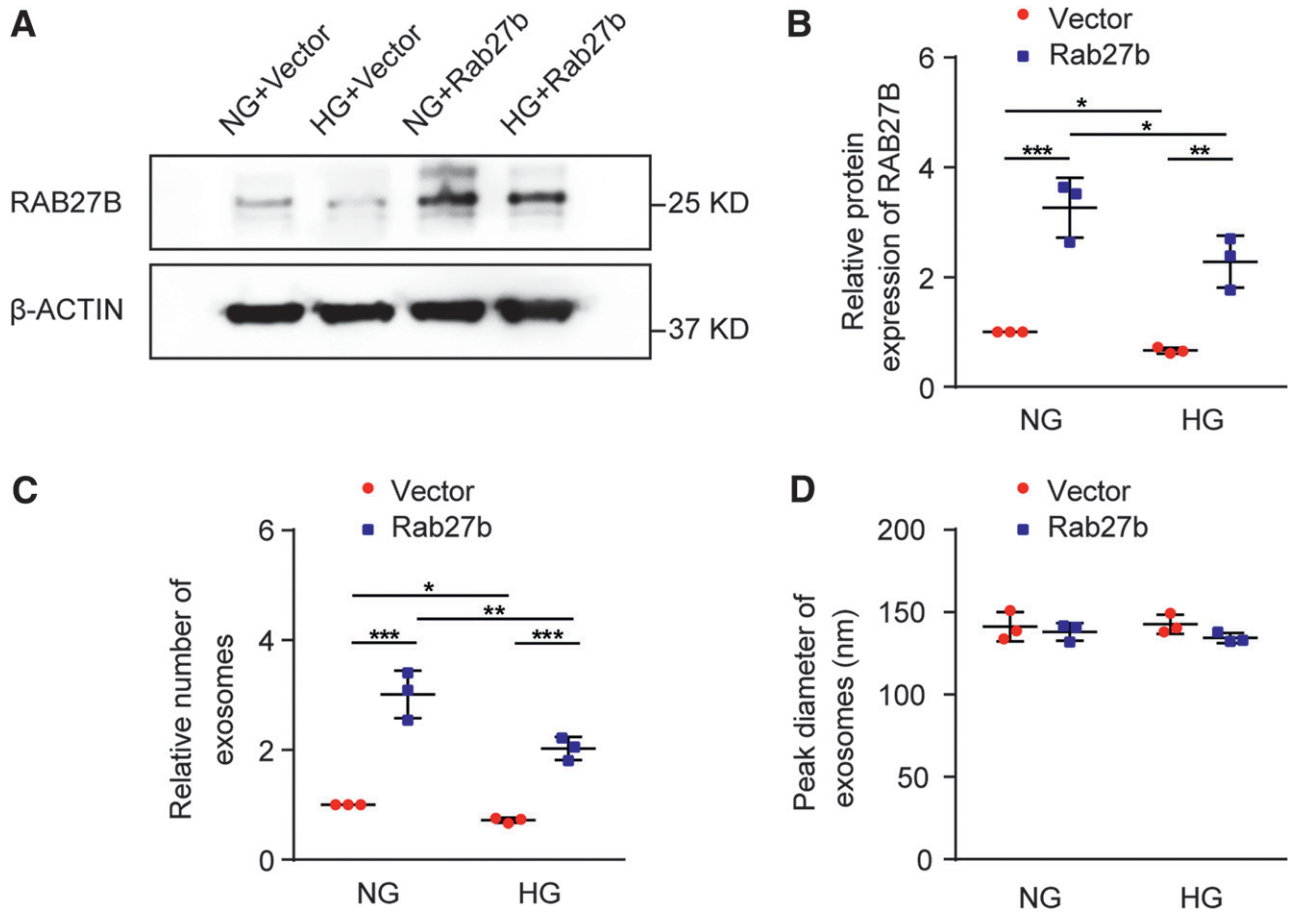

Figure 3—Overexpression of RAB27B restores exosome secretion in HG-incubated cells. BUMPT cells were stably transfected with Rab27b or empty vector plasmids. The cells were then cultured in medium containing 30 mmol/L glucose (HG) or 5.5 mmol/L glucose with 24.5 mmol/L D-mannitol (NG) to collect whole cell lysates for immunoblot analysis of RAB27B. Culture medium was collected for isolation and analysis of exosomes. *A*: Representative blots of RAB27B and β-actin (loading control). *B*: Densitometric analysis of RAB27B. After normalization with β-actin, the protein level in BUMPT cells stably transfected with the empty vector under the NG condition was arbitrarily set as 1, and the protein level in the other groups was compared with that 1 to calculate the fold change. $*P < 0.05$, $**P < 0.01$, $***P < 0.001$ ($n = 3$). *C*: RAB27B overexpression restored exosome secretion in BUMPT cells under the HG condition. Exosomes isolated from different conditions were analyzed with NTA for quantification. The exosome numbers were then normalized with cell counts. The number of exosomes released by empty vector-transfected BUMPT cells under the NG condition was arbitrarily set as 1, and the number of exosomes released by the other groups was compared with that 1 to calculate the fold change. $*P < 0.05$, $**P < 0.01$, $***P < 0.001$ ($n = 3$). *D*: RAB27B overexpression did not change the size of exosomes. The peak diameter of exosomes was determined by NTA ($n = 3$).

diabetic mice compared with control mice, whereas there was no significant difference in the sizes of exosomes between these two groups (Fig. 7*A* and *B*). In immunoblot analysis, diabetic mice had higher FOXO1 phosphorylation and lower expression of RAB27B in renal cortical tissues than control mice (Fig. 7*C*–*I*). The expression of other proteins involved in exosome biogenesis and secretion, including RAB27A, was not significantly altered by STZ-induced diabetes. DKD-associated decrease in RAB27B expression was further verified by immunostaining (Fig. 7*J* and *K*). Moreover, quantitative real-time PCR demonstrated lower mRNA of Rab27b in renal cortical tissues of diabetic mice than those of control mice (Fig. 7*M*). Similar results were shown for renal cortical tissues of diabetic Akita mice (Supplementary Fig. 3) and *db*/*db* mice (Supplementary Fig. 4). Taken together, these data indicate the correlation of FOXO1 phosphorylation/inactivation, RAB27B repression, and decreased exosome secretion in diabetic kidneys.

Rab27b Is Downregulated in Human Diabetic Kidneys and Negatively Associated With eGFR

Data were obtained from Nephroseq database (https://www.nephroseq.org). Microarray analysis showed a decreased mRNA level of Rab27b in the glomerulus and tubulointerstitium of DKD patients compared with healthy donors (Supplementary Fig. 5*A* and *B*). Besides, the Rab27b mRNA level in the tubulointerstitium of DKD patients was negatively associated with the eGFR based on the MDRD equation (Supplementary Fig. 5*C*).

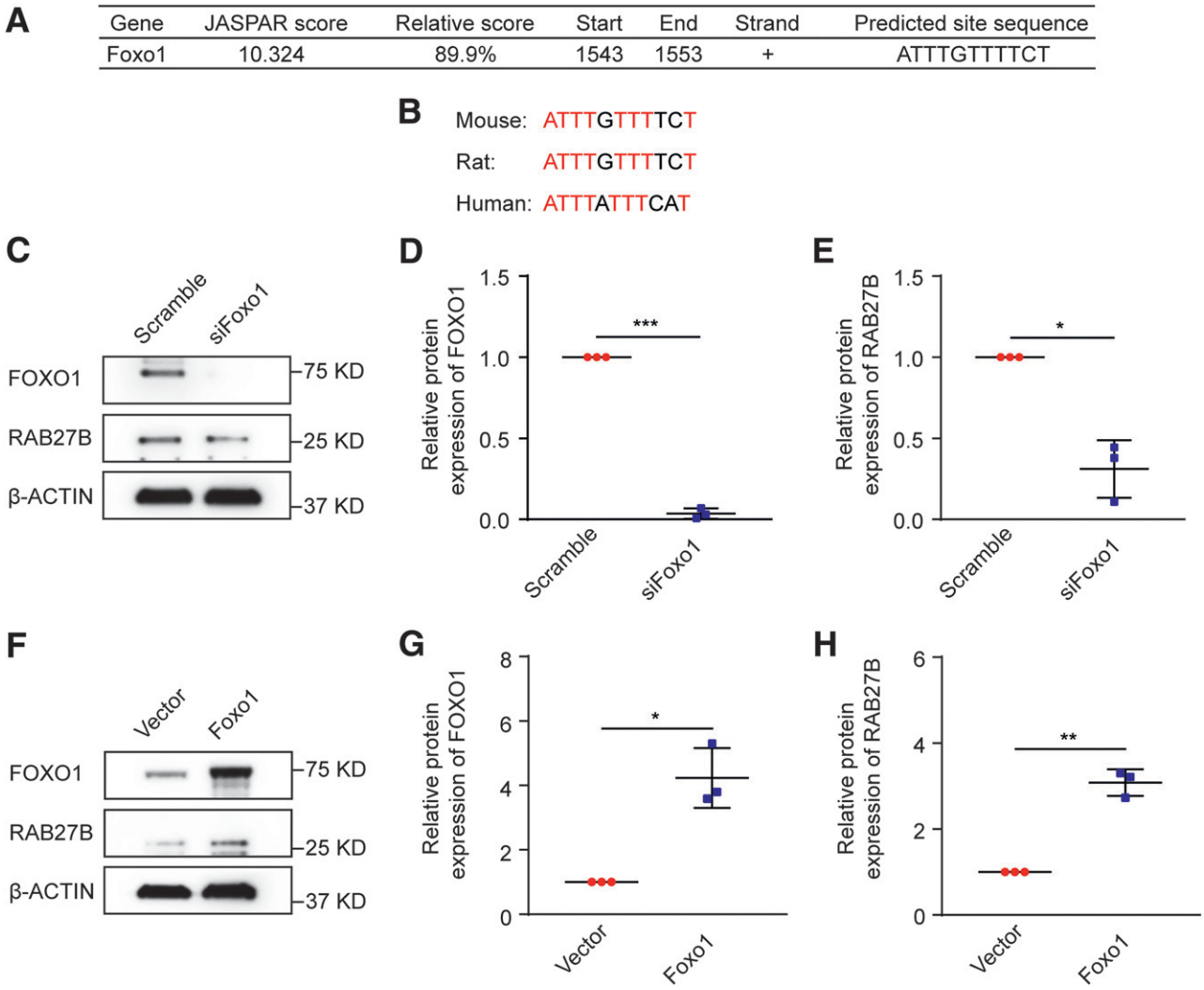

Figure 4—Regulation of RAB27B by FOXO1 in BUMPT cells. BUMPT cells were transiently transfected with siRNA or plasmid. Cell lysates were collected 48 h later for immunoblot analysis. *A*: Predicted FOXO1 binding site in the mouse Rab27b gene promoter region. The 5' region of the mouse Rab27b gene was analyzed for FOXO1 binding sites using the JASPAR database (https://jaspar.genereg.net). The binding site with a JASPAR score >10 was listed. *B*: Conservation of the predicted FOXO1 binding site in mouse, rat, and human genomes. Bases in common among different species are colored red. *C–E*: Knockdown of FOXO1 decreased RAB27B expression. BUMPT cells were transiently transfected with Foxo1 siRNA or scrambled sequence siRNA to collect cell lysates for immunoblot analysis. *C*: Representative immunoblots of FOXO1 and RAB27B. Densitometric analyses of FOXO1 (*D*) and RAB27B (*E*). β-Actin was used as the loading control. After normalization with β-actin, the protein level in the scramble group was arbitrarily set as 1, and the protein level in the siFoxo1 group was compared with that 1 to calculate the fold change. $*P < 0.05$, $***P < 0.001$ ($n = 3$). *F–H*: Nonphosphorylatable, constitutively active FOXO1 increased RAB27B expression. BUMPT cells were transiently transfected with empty vector or the plasmid of nonphosphorylatable, constitutively active Foxo1 to collect cell lysates for immunoblot analysis. *F*: Representative immunoblots of FOXO1 and RAB27B. Densitometric analyses of FOXO1 (*G*) and RAB27B (*H*). β-Actin was used as loading control. After normalization with β-actin, the protein level in the empty vector group was arbitrarily set as 1, and the protein level in the Foxo1 overexpression group was compared with that 1 to calculate the fold change. $*P < 0.05$, $**P < 0.01$ ($n = 3$).

DISCUSSION

Emerging evidence has implicated exosomes as a mode of intercellular communication in DKD, but the regulation of exosomes in DKD is largely unclear. In the current study, we have verified the significant decrease of exosome secretion in DKD using in vivo and in vitro models. Importantly, we show that this decrease results from the downregulation of RAB27B, a key RAB GTPase in exosome secretion. Our work further demonstrates a critical role of FOXO1 in the downregulation of RAB27B in DKD. In normal nondiabetic conditions, FOXO1 accumulates in the nucleus to induce the transcription or expression of RAB27B promoting exosome secretion. In diabetes, kidney cells and tissues are exposed to HG or hyperglycemia that induces the phosphorylation and cytosolic retention of FOXO1, preventing its nuclear accumulation and consequent transactivation and expression of RAB27B leading to the decrease of exosome secretion (Fig. 8). These findings unveil a novel mechanism that is

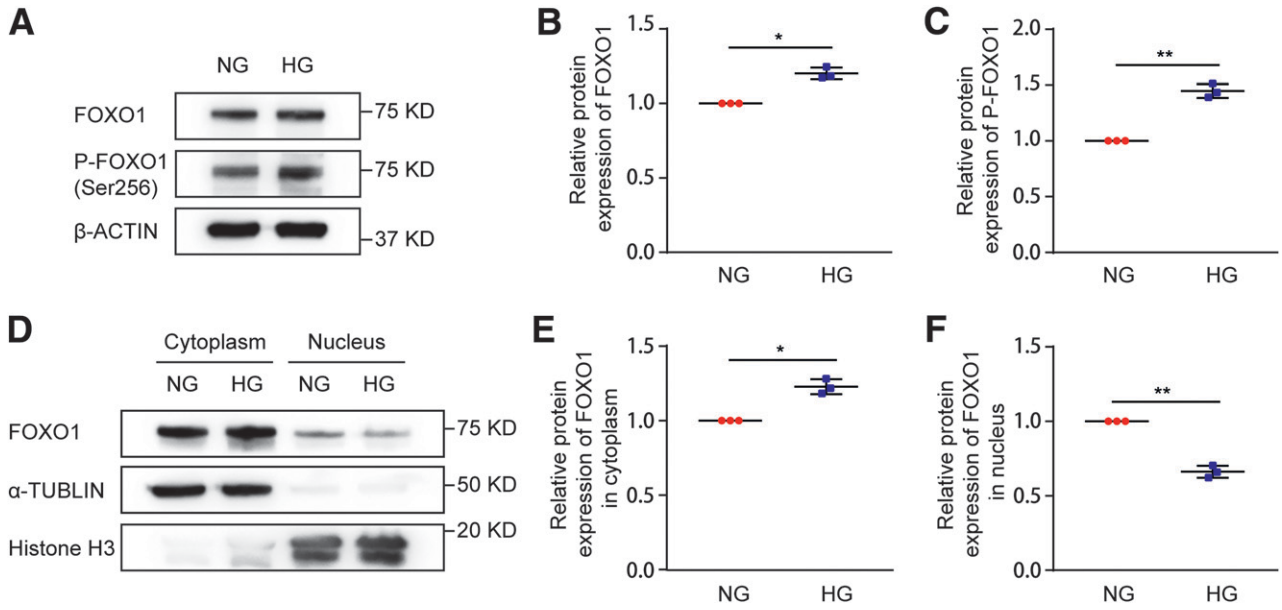

Figure 5—HG induces FOXO1 phosphorylation and inactivation in BUMPT cells. BUMPT cells were cultured in DMEM containing 30 mmol/L glucose (HG) or 5.5 mmol/L glucose with 24.5 mmol/L D-mannitol (NG) for 8 days. Cell lysates and subcellular fractions were collected at the end of the 8th day for immunoblot analysis. *A*: Increased FOXO1 phosphorylation in HG-treated cells. Representative immunoblots of total FOXO1 and p-FOXO1 (Ser256) in cell lysates from the NG and HG groups. *B*: Densitometric analysis of total FOXO1 in NG-treated and HG-treated cells. β-Actin was used as the loading control. After normalization with β-actin, the protein level in the NG group was arbitrarily set as 1, and the protein level in the HG group was compared with that 1 to calculate the fold change. $*P < 0.05$ ($n = 3$). *C*: Densitometric analysis of p-FOXO1 (Ser256) in NG-treated and HG-treated cells. Total FOXO1 was used as the loading control. After normalization with total FOXO1, the protein level in the NG group was arbitrarily set as 1, and the protein level in the HG group was compared with that 1 to calculate the fold change. $**P < 0.01$ ($n = 3$). *D–F*: Less nuclear FOXO1 in HG-treated cells than in NG-treated cells. Histone H3 and α-tubulin were probed as respective controls for nuclear and cytoplasmic fractions. *D*: Representative immunoblots of total FOXO1 in cytoplasmic and nuclear fractions of NG-treated and HG-treated cells. *E*: Densitometric analysis of cytoplasmic FOXO1 in NG-treated and HG-treated cells. After normalization with α-tubulin, the protein level in NG-treated cells was arbitrarily set as 1, and the protein level in the HG group was compared with that 1 to calculate the fold change. $*P < 0.05$ ($n = 3$). *F*: Densitometric analysis of nuclear FOXO1 in NG-treated and HG-treated cells. After normalization with histone H3, the protein level in NG-treated cells was arbitrarily set as 1, and the protein level in the HG group was compared with that 1 to calculate the fold change. $**P < 0.01$ ($n = 3$).

responsible for the decrease of exosome secretion in DKD and probably other diabetic complications.

Our recent study demonstrated the first evidence of decreased exosome secretion in DKD (37). The current study further verified this finding by showing decreased exosome secretion in HG-treated BUMPT cells and in renal cortical tissues of STZ-induced diabetic mice. Functionally, our previous study suggested that the exosomes from HG-treated BUMPT cells have a higher ability for fibroblast activation than those from NG-treated cells. Especially, they induced higher proliferation in fibroblasts accompanied by the production of more fibrotic proteins. Therefore, DKD is associated with not only the decrease in exosome production in renal tubular cells but also a change in the content of exosomes. Further analysis of exosomal contents may reveal the molecular basis of profibrotic activity of the exosomes derived from DKD cells or tissues. In this regard, the recent study by Liu et al. (45) suggested that tubule-derived exosomes may contribute to renal fibrosis through shuttling sonic hedgehog ligands, although it is unknown whether the exosomes from DKD cells or tissues contain more of these ligands.

In this study, we focused on the impact of HG on exosome secretion in proximal tubular cells. Other studies investigated the impact of HG on exosome secretion in glomerular cells. Wu et al. (25) and Ling et al. (46) reported that HG-treated mouse glomerular endothelial cells secreted more exosomes than NG-treated ones. Likewise, da Silva Novaes et al. (47) showed that HG-treated human mesangial cells secreted more exosomes than NG-treated ones. According to those studies, the exosome secretion in HG-treated glomerular cells is increased. Therefore, the impact of HG on exosome secretion may be divergent in different types of cells in kidneys.

To understand the mechanism of decreased exosome production in DKD models, we analyzed the proteins involved in exosome biogenesis and secretion. It is interesting that RAB27B was downregulated in both HG-treated BUMPT cells and in renal cortical tissues of STZ-treated mice, whereas there were no significant changes in the expression of ALIX, TSG101, and RAB27A (Figs. 2 and 7). ALIX and TSG101, belonging to the ESCRT machinery and are involved in the regulation of exosome biogenesis, whereas RAB27A and RAB27B are two small

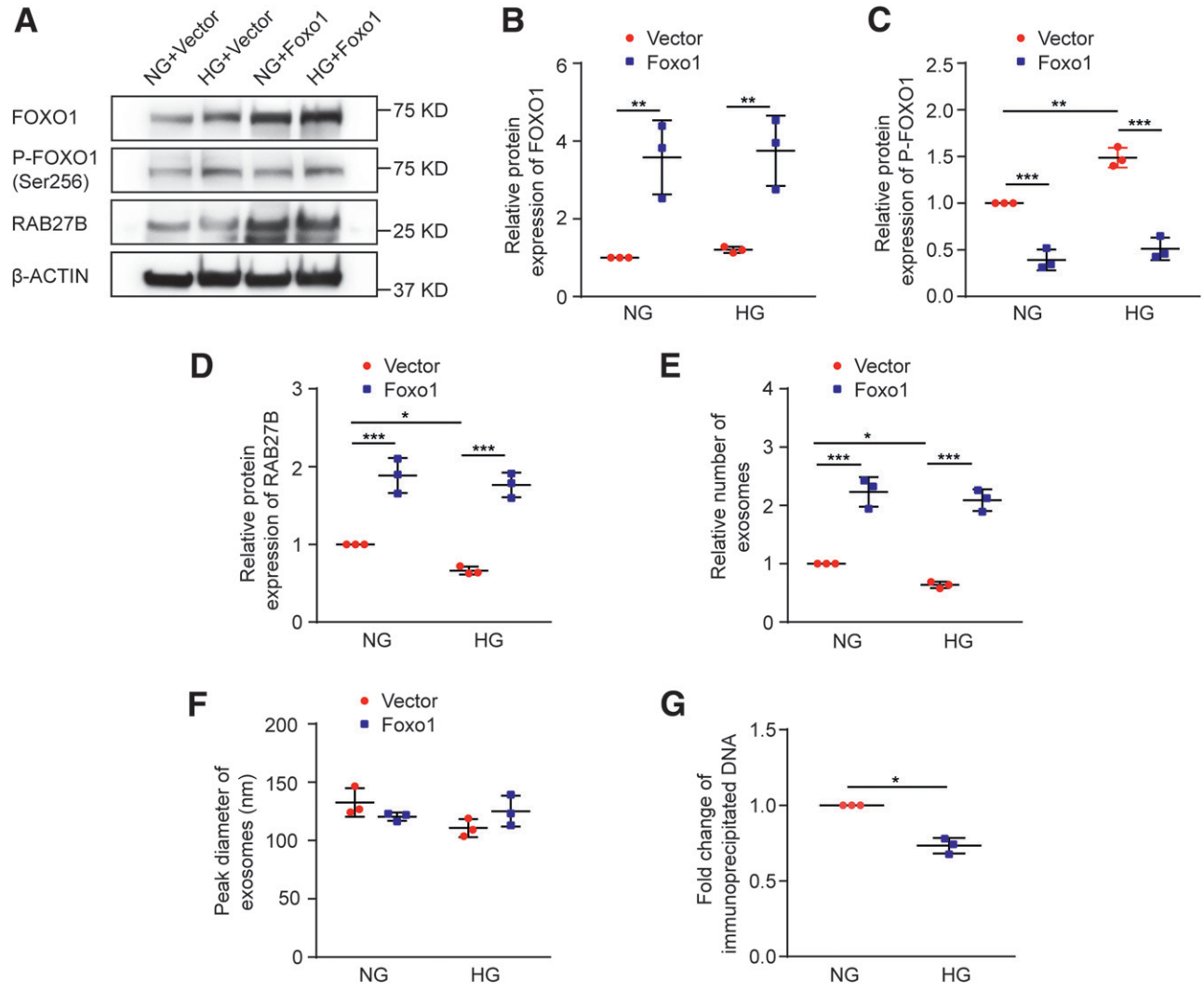

Figure 6—Regulation of RAB27B by FOXO1 affects exosome secretion in BUMPT cells under the HG condition. BUMPT cells were stably transfected with nonphosphorylatable, constitutively active FOXO1 or control empty vector. The cells were then cultured in DMEM containing 30 mmol/L glucose (HG) or 5.5 mmol/L glucose with 24.5 mmol/L D-mannitol (NG) for 8 days. Cell lysates and culture medium were collected at the end of the 8th day. Exosomes were isolated from the cell culture medium. *A–D*: Overexpression of nonphosphorylatable, constitutively active FOXO1 increased RAB27B expression. *A*: Representative immunoblots of total FOXO1, p-FOXO1 (Ser256), and RAB27B. *B*: Densitometric analysis of total FOXO1. β-Actin was used as the loading control. After normalization with β-actin, the protein level in BUMPT cells stably transfected with the empty vector under NG condition was arbitrarily set as 1, and the protein level in the other groups was compared with that 1 to calculate the fold change. $^{**}P < 0.01$ ($n = 3$). *C*: Densitometric analysis of p-FOXO1 (Ser256). The signal of p-FOXO1 was normalized by that of total FOXO1. After that, the protein level in BUMPT cells stably transfected with the empty vector under the NG condition was arbitrarily set as 1, and the protein level in the other groups was compared with that 1 to calculate the fold change. $^{**}P < 0.01$, $^{***}P < 0.001$ ($n = 3$). *D*: Densitometric analysis of RAB27B. β-Actin was used as the loading control. After normalization with β-actin, the protein level in BUMPT cells stably transfected with the empty vector under the NG condition was arbitrarily set as 1, and the protein level in the other groups was compared with that 1 to calculate the fold change. $^{*}P < 0.05$, $^{***}P < 0.001$ ($n = 3$). *E*: Nonphosphorylatable, active FOXO1 restored exosome secretion in BUMPT cells under the HG condition. The relative number of exosomes in four groups was based on quantification by NTA after normalization with cell counts. The number of exosomes released by BUMPT cells stably transfected with the empty vector under the NG condition was arbitrarily set as 1, and the number of exosomes released by the other groups was compared with that 1 to calculate the fold change. $^{*}P < 0.05$, $^{***}P < 0.001$ ($n = 3$). *F*: Nonphosphorylatable, active FOXO1 did not change the size of exosomes under the HG condition. The peak diameter of exosomes was analyzed by NTA ($n = 3$). *G*: Decreased binding of FOXO1 to the Rab27b promoter sequence in HG-treated cells. BUMPT cells were cultured in DMEM containing 30 mmol/L glucose (HG) or 5.5 mmol/L glucose with 24.5 mmol/L D-mannitol (NG) for 8 days for ChIP assay using anti-FOXO1 antibody. The values were normalized to that of the NG group, which was arbitrarily set at 1. $^{*}P < 0.05$ ($n = 3$).

GTPases in the late endosomal compartment that play critical roles in exosome secretion (11). Our results suggest that DKD is not associated with an overall shutdown of the exosomal biogenesis machinery but with a specific downregulation of the exosome secretion regulator RAB27B. Notably, overexpression of RAB27B restored exosome

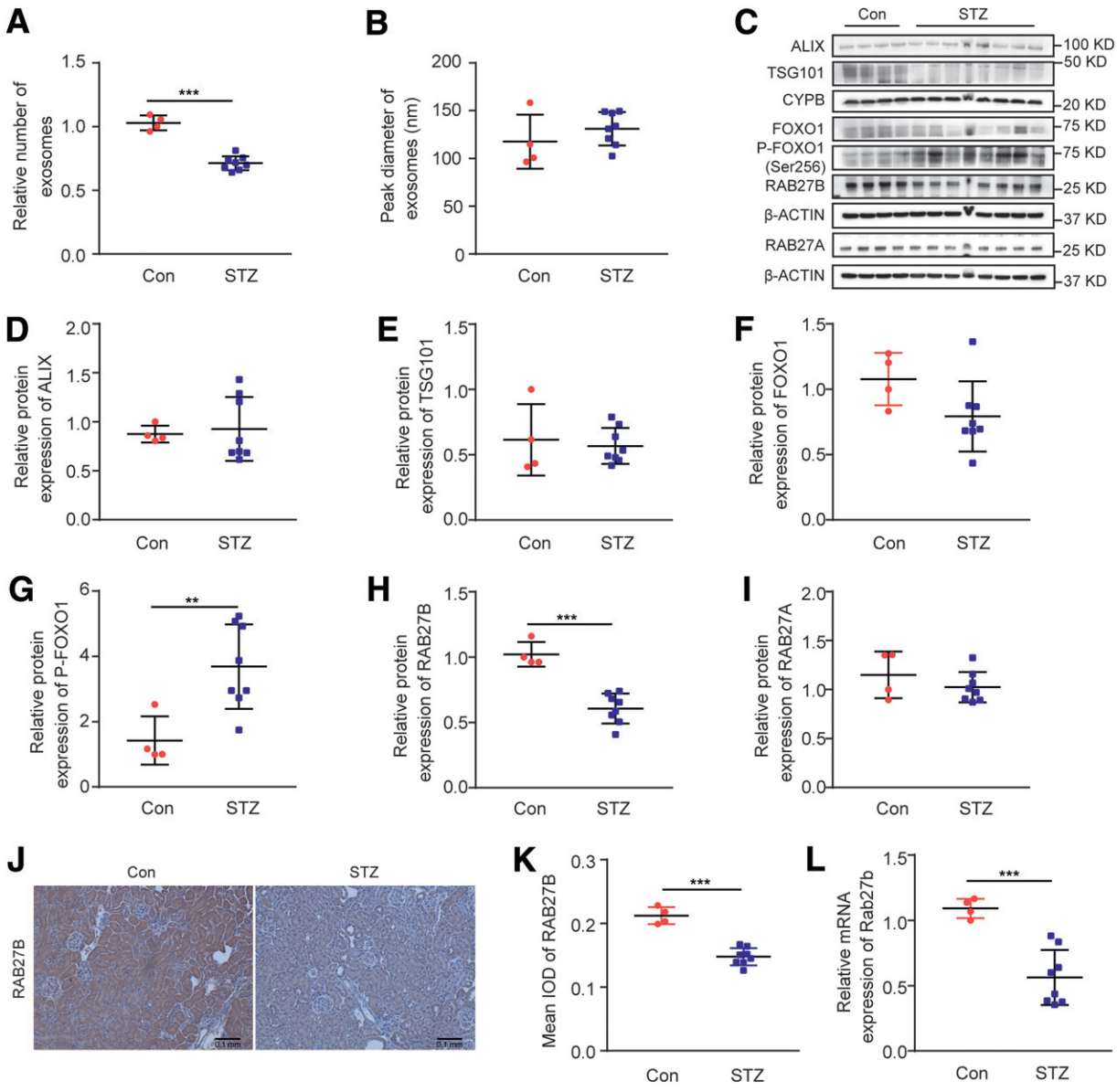

Figure 7—FOXO1 phosphorylation, RAB27B downregulation, and decreased exosome secretion in renal cortical tissues of STZ-induced diabetic mice. C57BL/6J male mice (8 weeks) were treated with STZ to induce diabetes or with vehicle solution as the control (Con). The mice were sacrificed at 20 weeks of age to collect renal cortical tissues. *A*: Diabetic mice produced fewer exosomes in renal cortical tissues than nondiabetic mice. The relative number of exosomes in the control ($n = 4$) and STZ ($n = 8$) groups was based on quantification by NTA from equal weights of renal cortical tissues. ***$P < 0.001$. *B*: No significant difference in the sizes of exosomes isolated from renal cortical tissues of nondiabetic mice and diabetic mice. Peak diameter of exosomes was analyzed by NTA in control ($n = 4$) and STZ ($n = 8$) groups. *C–I*: Increased FOXO1 phosphorylation and decreased RAB27B expression in renal cortical tissues of diabetic mice. *C*: Representative immunoblots of ALIX, TSG101, FOXO1, p-FOXO1 (Ser256), RAB27B, and RAB27A. Densitometric analyses of ALIX (*D*) and TSG101 (*E*) in the control ($n = 4$) and STZ ($n = 8$) groups. Cyclophilin B was used as the loading control. After normalization with cyclophilin B, the protein level of the control group was arbitrarily set as 1, and the protein level of other mice was compared with it to calculate the fold change. *F*: Densitometric analysis of total FOXO1 in the control ($n = 4$) and STZ ($n = 8$) groups. β-Actin was used as the loading control. After normalization with β-actin, the protein level of the control group was arbitrarily set as 1, and the protein level of the other mice was compared with it to calculate the fold change. *G*: Densitometric analysis of p-FOXO1 (Ser256) in the control ($n = 4$) and STZ ($n = 8$) groups. p-FOXO1 was normalized with total FOXO1. After normalization, the protein level of the control group was arbitrarily set as 1, and the protein level of other mice was compared with it to calculate the fold change. **$P < 0.01$. Densitometric analyses of RAB27B (*H*) and RAB27A (*I*) in the control ($n = 4$) and STZ ($n = 8$) groups. β-Actin was used as the loading control. After normalization with β-actin, the protein level of the control group was arbitrarily set as 1, and the protein level of other mice was compared with it to calculate the fold change. ***$P < 0.001$. *J* and *K*: Immunohistochemistry showing decreased RAB27B expression in diabetic mouse kidneys. *J*: Representative immunohistochemistry images. Original magnification ×10; scale bar, 0.1 mm. *K*: Quantitative analysis of RAB27B staining by Image-Pro Plus in the control ($n = 4$) and STZ ($n = 8$) groups. ***$P < 0.001$. *M*: Decreased mRNA level of Rab27b in renal cortical tissues of diabetic mice. The mRNA level of Rab27b was detected by real-time PCR in the control ($n = 4$) and STZ ($n = 8$) groups. β-Actin was used as the reference gene. After normalization with β-actin, the mRNA level of the control group was arbitrarily set as 1, and the mRNA levels of the other mice were compared with it to calculate the fold change. ***$P < 0.001$.

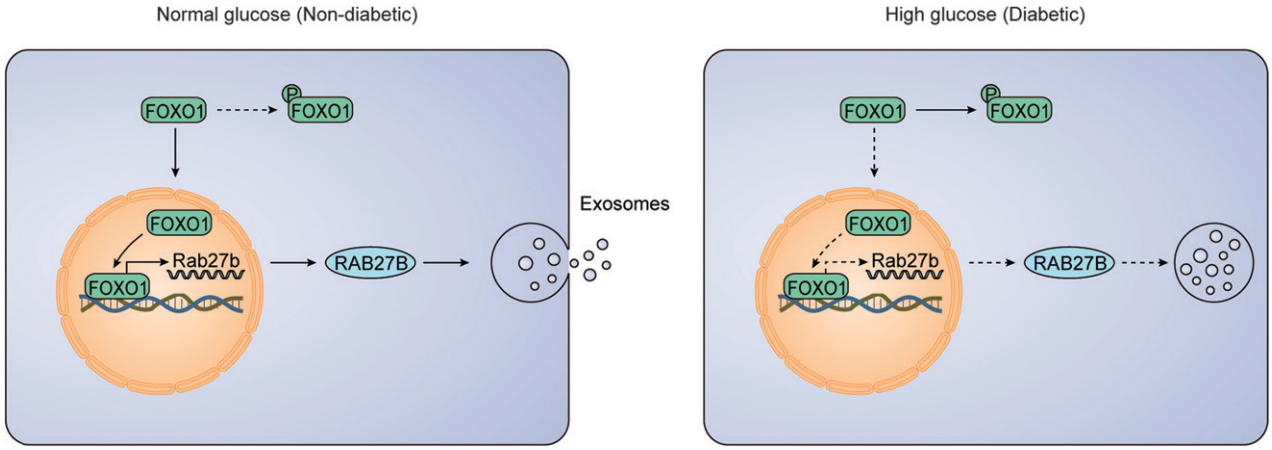

Figure 8—Schematic diagram depicting the FOXO1/RAB27B pathway for decreased exosome secretion in diabetic kidneys. Normally, FOXO1 accumulates in the nucleus to induce gene transcription and expression of RAB27B, promoting exosome secretion. In diabetic kidney cells and tissues, HG induces the phosphorylation and cytosolic retention of FOXO1, which prevents the transactivation and expression of RAB27B and leads to the decrease of exosome secretion.

secretion in HG-treated cells (Fig. 3), suggesting that downregulation of RAB27B may be the cause of decreased exosome secretion in DKD. To our knowledge, this is the first evidence that RAB27B is repressed, accounting for decreased exosome secretion in diabetic kidneys.

What leads to RAB27B downregulation in DKD? To address this, our initial analysis showed that HG incubation reduced Rab27b mRNA expression in cells (Fig. 2*F*), indicating a possible repression of RAB27B at the transcriptional level. Wheras HG incubation led to RAB27B repression, TGF-β1 treatment did not affect RAB27B expression in BUMPT cells (Supplementary Fig. 6). We further analyzed its gene promoter and identified putative FOXO1 binding sites. Interestingly, Das et al. (44) reported the phosphorylation and inactivation of FOXO1 in DKD. With this information, we examined whether FOXO1 inactivation could be the cause of RAB27B downregulation in DKD. Our results show that knockdown of FOXO1 decreased RAB27B expression in BUMPT cells, whereas overexpression of FOXO1 had the opposite effect, indicating that RAB27B is subjected to FOXO1 regulation in renal tubular cells. FOXO1 is a forkhead transcription factor that plays vital roles in the regulation of various cellular functions, including proliferation, apoptosis, metabolism, oxidative stress, atrophy, and inflammation (48).

Several transcription factors have been shown to regulate RAB27B under different experimental conditions. For example, Tiwari et al. (49) reported the recruitment of NF-E2 to the Rab27b gene promoter by ChIP assay in primary murine megakaryocytes, suggesting that RAB27B may be a direct transcriptional target of NF-E2. More recently, Yang et al. (50) demonstrated the transcriptional regulation of RAB27B by CREB in human pancreatic cancer cells. Our current study uncovers a previously uncharacterized FOXO1-RAB27B signaling pathway in renal tubular cells in DKD.

An important mechanism that regulates the transcriptional activity of FOXO1 is phosphorylation. In T1DM OVE26 mice, Das et al. (44) demonstrated a significant increase of FOXO1 phosphorylation that was associated with a decrease in catalase expression and increases in fibrotic protein expression. Consistently, our present study showed a significant FOXO1 phosphorylation in HG-treated BUMPT cells and in renal cortical tissues of STZ-treated mice (Figs. 5 and 7). We further demonstrated less FOXO1 accumulation in the nucleus of HG-treated BUMPT cells. This observation is in line with the current understanding of FOXO1 regulation. It has been reported that phosphorylation of FOXO1 is closely associated with its nuclear export and promotes FOXO1 nuclear exclusion, resulting in weakened transcriptional activities (51). In our study, overexpression of nonphosphorylatable, constitutively active FOXO1 led to the upregulation of RAB27B and increase in exosome secretion in HG-treated BUMPT cells (Fig. 6), further supporting the scenario that phosphorylation of FOXO1 in DKD may result in decreased transcription and expression of RAB27B, leading to decreased exosome secretion.

Acknowledgments. The authors thank Dr. David Stepp's laboratory at the Vascular Biology Center of Augusta University for providing the kidney tissues of *db*/*db* mice.

Funding. This study was supported in part by grants from the U.S. Department of Veterans Affairs (Merit Review Award I01 BX000319) and the National Institutes of Health National Institute of Diabetes and Digestive and Kidney Diseases (DK058831 and DK087843). Z.D. is a recipient of Senior Research Career Scientist award from the U.S. Department of Veterans Affairs.

Duality of Interest. No potential conflicts of interest relevant to this article were reported.

Author Contributions. M.Z. drafted the manuscript. M.Z., J.W., and Z.M. conducted experiments. M.Z., J.W., Z.M., L.X., Yut.L., S.K., Yu.L., and Z.D. contributed to data analysis and interpretation. M.Z. and Z.D. designed

the study. L.X. and Z.D. revised the manuscript. All authors read and approved the final manuscript. M.Z. is the guarantor of this work and, as such, had full access to all the data in the study and takes responsibility for the integrity of the data and the accuracy of the data analysis.

Prior Presentation. Parts of this study were presented in abstract form at the American Society of Nephrology Kidney Week 2020 digital meeting, 19–21 October 2020.

References

1. Doyle LM, Wang MZ. Overview of extracellular vesicles, their origin, composition, purpose, and methods for exosome isolation and analysis. Cells 2019; 8:E727
2. Kalluri R, LeBleu VS. The biology, function, and biomedical applications of exosomes. Science 2020;367:eaau6977
3. Zhang W, Zhou X, Zhang H, Yao Q, Liu Y, Dong Z. Extracellular vesicles in diagnosis and therapy of kidney diseases. Am J Physiol Renal Physiol 2016; 311:F844–F851
4. Zhang W, Zhou X, Yao Q, Liu Y, Zhang H, Dong Z. HIF-1-mediated production of exosomes during hypoxia is protective in renal tubular cells. Am J Physiol Renal Physiol 2017;313:F906–F913
5. Karpman D, Ståhl AL, Arvidsson I. Extracellular vesicles in renal disease. Nat Rev Nephrol 2017;13:545–562
6. Dominguez JH, Liu Y, Gao H, Dominguez JM II, Xie D, Kelly KJ. Renal tubular cell-derived extracellular vesicles accelerate the recovery of established renal ischemia reperfusion injury. J Am Soc Nephrol 2017;28:3533–3544
7. Lv LL, Feng Y, Wen Y, et al. Exosomal CCL2 from tubular epithelial cells is critical for albumin-induced tubulointerstitial inflammation. J Am Soc Nephrol 2018;29:919–935
8. Li ZL, Lv LL, Tang TT, et al. HIF-1α inducing exosomal microRNA-23a expression mediates the cross-talk between tubular epithelial cells and macrophages in tubulointerstitial inflammation. Kidney Int 2019;95:388–404
9. van Niel G, D'Angelo G, Raposo G. Shedding light on the cell biology of extracellular vesicles. Nat Rev Mol Cell Biol 2018;19:213–228
10. Schmidt O, Teis D. The ESCRT machinery. Curr Biol 2012;22:R116–R120
11. Kowal J, Tkach M, Théry C. Biogenesis and secretion of exosomes. Curr Opin Cell Biol 2014;29:116–125
12. Tuttle KR, Bakris GL, Bilous RW, et al. Diabetic kidney disease: a report from an ADA Consensus Conference. Am J Kidney Dis 2014;64:510–533
13. Stanton RC. Clinical challenges in diagnosis and management of diabetic kidney disease. Am J Kidney Dis 2014;63(Suppl. 2):S3–S21
14. Zhang L, Long J, Jiang W, et al. Trends in chronic kidney disease in China. N Engl J Med 2016;375:905–906
15. Ma Z, Li L, Livingston MJ, et al. p53/microRNA-214/ULK1 axis impairs renal tubular autophagy in diabetic kidney disease. J Clin Invest 2020;130: 5011–5026
16. Yao Y, Wang J, Yoshida S, Nada S, Okada M, Inoki K. Role of ragulator in the regulation of mechanistic target of rapamycin signaling in podocytes and glomerular function. J Am Soc Nephrol 2016;27:3653–3665
17. Fan Y, Yi Z, D'Agati VD, et al. Comparison of kidney transcriptomic profiles of early and advanced diabetic nephropathy reveals potential new mechanisms for disease progression. Diabetes 2019;68:2301–2314
18. Kato M, Natarajan R. Epigenetics and epigenomics in diabetic kidney disease and metabolic memory. Nat Rev Nephrol 2019;15:327–345
19. Fu J, Akat KM, Sun Z, et al. Single-cell RNA profiling of glomerular cells shows dynamic changes in experimental diabetic kidney disease. J Am Soc Nephrol 2019;30:533–545
20. Doi T, Moriya T, Fujita Y, et al. Urinary IgG4 and Smad1 are specific biomarkers for renal structural and functional changes in early stages of diabetic nephropathy. Diabetes 2018;67:986–993
21. Chauhan K, Verghese DA, Rao V, et al. Plasma endostatin predicts kidney outcomes in patients with type 2 diabetes. Kidney Int 2019;95:439–446
22. Chertow GM, Pergola PE, Chen F, Kirby BJ, Sundy JS; GS-US-223-1015 Investigators. Effects of selonsertib in patients with diabetic kidney disease. J Am Soc Nephrol 2019;30:1980–1990
23. Mann JFE, Fonseca VA, Poulter NR, et al.; LEADER Trial Investigators. Safety of liraglutide in type 2 diabetes and chronic kidney disease. Clin J Am Soc Nephrol 2020;15:465–473
24. Liang X, Wang P, Chen B, et al. Glycogen synthase kinase 3β hyperactivity in urinary exfoliated cells predicts progression of diabetic kidney disease. Kidney Int 2020;97:175–192
25. Wu X, Gao Y, Xu L, et al. Exosomes from high glucose-treated glomerular endothelial cells trigger the epithelial-mesenchymal transition and dysfunction of podocytes. Sci Rep 2017;7:9371
26. Zhu QJ, Zhu M, Xu XX, Meng XM, Wu YG. Exosomes from high glucose-treated macrophages activate glomerular mesangial cells *via* TGF-β1/Smad3 pathway *in vivo* and *in vitro*. FASEB J 2019;33:9279–9290
27. Zhu M, Sun X, Qi X, Xia L, Wu Y. Exosomes from high glucose-treated macrophages activate macrophages andinduce inflammatory responses via NF-κB signaling pathway in vitro and in vivo. Int Immunopharmacol 2020;84: 106551
28. Su H, Qiao J, Hu J, et al. Podocyte-derived extracellular vesicles mediate renal proximal tubule cells dedifferentiation via microRNA-221 in diabetic nephropathy. Mol Cell Endocrinol 2020;518:111034
29. Ebrahim N, Ahmed IA, Hussien NI, et al. Mesenchymal stem cell-derived exosomes ameliorated diabetic nephropathy by autophagy induction through the mTOR signaling pathway. Cells 2018;7:226
30. Jin J, Shi Y, Gong J, et al. Exosome secreted from adipose-derived stem cells attenuates diabetic nephropathy by promoting autophagy flux and inhibiting apoptosis in podocyte. Stem Cell Res Ther 2019;10:95
31. Duan YR, Chen BP, Chen F, et al. Exosomal microRNA-16-5p from human urine-derived stem cells ameliorates diabetic nephropathy through protection of podocyte. J Cell Mol Med. 30 September 2019 [Epub ahead of print]. DOI: 10.1111/jcmm.14558
32. Xiang E, Han B, Zhang Q, et al. Human umbilical cord-derived mesenchymal stem cells prevent the progression of early diabetic nephropathy through inhibiting inflammation and fibrosis. Stem Cell Res Ther 2020;11:336
33. Eissa S, Matboli M, Bekhet MM. Clinical verification of a novel urinary microRNA panal: 133b, -342 and -30 as biomarkers for diabetic nephropathy identified by bioinformatics analysis. Biomed Pharmacother 2016;83:92–99
34. De S, Kuwahara S, Hosojima M, et al. Exocytosis-mediated urinary full-length megalin excretion is linked with the pathogenesis of diabetic nephropathy. Diabetes 2017;66:1391–1404
35. Chang CC, Chen CY, Huang CH, et al. Urinary glycated uromodulin in diabetic kidney disease. Clin Sci (Lond) 2017;131:1815–1829
36. Yamamoto CM, Murakami T, Oakes ML, et al. Uromodulin mRNA from urinary extracellular vesicles correlate to kidney function decline in type 2 diabetes mellitus. Am J Nephrol 2018;47:283–291
37. Wen J, Ma Z, Livingston MJ, et al. Decreased secretion and profibrotic activity of tubular exosomes in diabetic kidney disease. Am J Physiol Renal Physiol 2020;319:F664–F673
38. Nakae J, Kitamura T, Silver DL, Accili D. The forkhead transcription factor Foxo1 (Fkhr) confers insulin sensitivity onto glucose-6-phosphatase expression. J Clin Invest 2001;108:1359–1367
39. Sinha D, Bannergee S, Schwartz JH, Lieberthal W, Levine JS. Inhibition of ligand-independent ERK1/2 activity in kidney proximal tubular cells deprived of soluble survival factors up-regulates Akt and prevents apoptosis. J Biol Chem 2004;279:10962–10972
40. Ma Z, Wei Q, Zhang M, Chen JK, Dong Z. Dicer deficiency in proximal tubules exacerbates renal injury and tubulointerstitial fibrosis and upregulates Smad2/3. Am J Physiol Renal Physiol 2018;315:F1822–F1832

41. Huang F, Wang Q, Guo F, et al. FoxO1-mediated inhibition of STAT1 alleviates tubulointerstitial fibrosis and tubule apoptosis in diabetic kidney disease. EBioMedicine 2019;48:491–504
42. Ji L, Wang Q, Huang F, et al. FOXO1 overexpression attenuates tubulointerstitial fibrosis and apoptosis in diabetic kidneys by ameliorating oxidative injury via TXNIP-TRX. Oxid Med Cell Longev 2019; 2019:3286928
43. Pan CW, Jin X, Zhao Y, et al. AKT-phosphorylated FOXO1 suppresses ERK activation and chemoresistance by disrupting IQGAP1-MAPK interaction. EMBO J 2017;36:995–1010
44. Das F, Ghosh-Choudhury N, Dey N, et al. High glucose forces a positive feedback loop connecting Akt kinase and FoxO1 transcription factor to activate mTORC1 kinase for mesangial cell hypertrophy and matrix protein expression. J Biol Chem 2014;289:32703–32716
45. Liu X, Miao J, Wang C, et al. Tubule-derived exosomes play a central role in fibroblast activation and kidney fibrosis. Kidney Int 2020;97:1181–1195
46. Ling L, Tan Z, Zhang C, et al. CircRNAs in exosomes from high glucose-treated glomerular endothelial cells activate mesangial cells. Am J Transl Res 2019;11:4667–4682
47. da Silva Novaes A, Borges FT, Maquigussa E, Varela VA, Dias MVS, Boim MA. Influence of high glucose on mesangial cell-derived exosome composition, secretion and cell communication. Sci Rep 2019;9:6270
48. Wang Y, Zhou Y, Graves DT. FOXO transcription factors: their clinical significance and regulation. BioMed Res Int 2014;2014:925350
49. Tiwari S, Italiano JE Jr., Barral DC, et al. A role for Rab27b in NF-E2-dependent pathways of platelet formation. Blood 2003;102:3970–3979
50. Yang J, Zhang Z, Zhang Y, et al. ZIP4 promotes muscle wasting and cachexia in mice with orthotopic pancreatic tumors by stimulating RAB27B-regulated release of extracellular vesicles from cancer cells. Gastroenterology 2019;156:722–734.e6
51. Boccitto M, Kalb RG. Regulation of Foxo-dependent transcription by post-translational modifications. Curr Drug Targets 2011;12:1303–1310